http://doi.org/10.35784/iapgos.7201 *received: 03.02.2025 | revised: 25.08.2025 | accepted: 18.11.2025 | available online: 20.12.2025*

ADVANCED ENERGY MANAGEMENT STRATEGIES FOR AC/DC MICROGRIDS

Zouhir Boumous[1], Samira Boumous[1], Tawfik Thelaidjia[2,3]
[1]University of Souk Ahras, Electrical Engineering Department, Laboratory of Electrical Engineering, Electronic and Renewable Energy, Souk Ahras, Algeria, [2]University of Tebessa, Electrical Engineering Research Laboratory, Tebessa, Algeria, [3]University of Souk Ahras, Electrical Engineering Department, Souk Ahras, Algeria

Abstract*. This article investigates the active and reactive power dynamics of a hybrid AC/DC microgrid, with a particular focus on coordinated energy management among photovoltaic (PV) systems, synchronous generators, fuel cells, batteries, and supercapacitors. The novelty of this work lies in the integrated evaluation of bidirectional power flow, transient response, and voltage stability, which are addressed simultaneously through detailed simulations. Unlike existing studies that mainly highlight steady-state operation or isolated component performance, our analysis provides a holistic view of component interaction under dynamic conditions. The PV unit is modeled with a triangular power profile, peaking at 7 kW within 200 seconds, thereby capturing realistic variability in solar generation. The synchronous generator consistently delivers around 5 kW, adapting its output to compensate for load fluctuations ranging from 5.5 to 9.5 kW. The fuel cell, with a minimum output of 2 kW, ensures continuous supply during low renewable periods. Energy storage elements demonstrate complementary roles: the battery alternates between charging and discharging cycles, while the supercapacitor mitigates fast power deviations in the range of −0.05 kW to 0.3 kW. On the reactive power side, the load demands between −0.95 kvar and −0.5 kvar, with the synchronous generator contributing −0.65 kvar and the voltage source converters (VSC1 and VSC2) providing additional dynamic support. Importantly, the battery and ultracapacitor maintain voltage stability at 431.665 V and 249.5 V, respectively. Overall, the findings validate the robustness and efficiency of the proposed hybrid microgrid strategy, highlighting its contribution to enhancing grid resilience, stability, and reliable energy flow management.*

Keywords: microgrid, AC/DC system, energy management, bidirectional power flow

ZAAWANSOWANE STRATEGIE ZARZĄDZANIA ENERGIĄ DLA MIKROSIECI AC/DC

Streszczenie*. Niniejszy artykuł bada dynamikę mocy czynnej i biernej hybrydowej mikrosieci AC/DC, ze szczególnym uwzględnieniem skoordynowanego zarządzania energią pomiędzy systemami fotowoltaicznymi (PV), generatorami synchronicznymi, ogniwami paliwowymi, bateriami i superkondensatorami. Nowość tej pracy polega na zintegrowanej ocenie dwukierunkowego przepływu mocy, odpowiedzi przejściowej i stabilności napięcia, które są rozpatrywane jednocześnie poprzez szczegółowe symulacje. W przeciwieństwie do istniejących badań, które podkreślają głównie działanie w stanie ustalonym lub izolowaną wydajność komponentów, nasza analiza zapewnia całościowy obraz interakcji komponentów w warunkach dynamicznych. Jednostka fotowoltaiczna jest modelowana z trójkątnym profilem mocy, osiągającym szczyt 7 kW w ciągu 200 sekund, co pozwala uchwycić realistyczną zmienność generacji energii słonecznej. Generator synchroniczny stale dostarcza około 5 kW, dostosowując swoją moc wyjściową w celu kompensacji wahań obciążenia w zakresie od 5,5 do 9,5 kW. Ogniwo paliwowe o minimalnej mocy wyjściowej 2 kW zapewnia ciągłe zasilanie w okresach niskiego poziomu energii odnawialnej. Elementy magazynujące energię pełnią uzupełniające się role: bateria na przemian ładuje się i rozładowuje, podczas gdy superkondensator łagodzi szybkie odchylenia mocy w zakresie od –0,05 kW do 0,3 kW. Po stronie mocy biernej obciążenie wymaga od –0,95 kvar do –0,5 kvar, przy czym generator synchroniczny wnosi –0,65 kvar, a przetwornice źródła napięcia (VSC1 i VSC2) zapewniają dodatkowe wsparcie dynamiczne. Co ważne, bateria i ultrakondensator utrzymują stabilność napięcia na poziomie odpowiednio 431,665 V i 249,5 V. Ogólnie rzecz biorąc, wyniki badań potwierdzają solidność i wydajność proponowanej strategii hybrydowej mikrosieci, podkreślając jej wkład w zwiększanie odporności sieci, stabilności i niezawodnego zarządzania przepływem energii.*

Słowa kluczowe: mikrosieć, system AC/DC, zarządzanie energią, dwukierunkowy przepływ mocy

Introduction

The increasing demand for sustainable and efficient energy systems has driven the development of hybrid AC/DC microgrids, which integrate renewable energy sources, energy storage systems, and advanced power electronics [4, 9, 11]. These microgrids offer significant advantages over traditional grids by providing a flexible and decentralized platform for energy generation, storage, and distribution [21, 25]. A key enabler of this flexibility is the bidirectional power flow capability facilitated by voltage source converters (VSCs), which serve as the critical interface between the AC and DC subsystems [7, 13, 20]. VSCs ensure efficient coupling of these two domains, allowing power to flow seamlessly in either direction based on system requirements [18]. This functionality not only enhances energy efficiency but also prioritizes the utilization of renewable energy sources, thereby reducing reliance on fossil fuels and supporting grid stability [23].

In hybrid microgrids, the integration of renewable energy sources such as solar photovoltaic (PV) systems and wind turbines introduces variability and intermittency into the energy supply [24]. To address these challenges, energy storage systems like batteries and ultracapacitors are deployed to store excess energy during periods of high generation and release it during periods of low generation or high demand. The DC side of the microgrid typically accommodates these renewable energy sources and storage systems, offering a stable and efficient platform for energy management. On the other hand, the AC side supports traditional loads, synchronous generators, and grid connections, enabling the microgrid to operate in both grid-connected and islanded modes. The bidirectional power flow through VSCs ensures that energy can be efficiently exchanged between these two domains, maintaining system balance and stability even under dynamic operating conditions [14, 16].

Advanced control strategies and optimization techniques further enhance the performance of VSCs in hybrid microgrids. These control systems enable real-time power flow adjustments, voltage regulation, and frequency stabilization, ensuring that the microgrid operates reliably and efficiently. By enabling the seamless integration of renewable energy sources and managing the interaction between AC and DC systems, VSCs play a pivotal role in optimizing energy utilization and improving overall grid resilience [28].

The evolution of hybrid AC/DC microgrids has been driven by advancements in renewable energy, energy storage, and power electronics over the past few decades. Initially developed in the 1970s for isolated grids in remote areas, microgrids evolved with the integration of renewable sources like solar and wind in the 1990s, alongside the development of voltage source converters (VSCs) to couple AC and DC systems [3]. The 2000s saw the proliferation of lithium-ion batteries and ultracapacitors, enabling efficient energy storage and management, while energy management systems (EMS) were introduced to optimize power flow and grid stability [12]. In the modern era, hybrid microgrids incorporate smart grid technologies, IoT, and advanced control methods like predictive algorithms and machine learning, with increasing focus on hydrogen systems and hybrid energy storage for flexibility and resilience [15, 19, 26]. Today, hybrid AC/DC microgrids are central to sustainable energy strategies, balancing renewable integration, grid reliability, and decentralized

energy solutions [2, 27, 31]. The main objective of this study is to analyze the active and reactive power dynamics of a hybrid AC/DC microgrid, with a particular focus on the coordinated operation of photovoltaic (PV) systems, fuel cells, synchronous generators, batteries, and supercapacitors, in order to ensure stability, reliability, and efficient energy management under dynamic conditions. The research aims to enhance the overall energy management of hybrid microgrids by ensuring efficient power exchange between the AC and DC sides, improving grid stability, and maximizing the utilization of renewable energy. By employing advanced energy optimization techniques, the study seeks to minimize energy losses, balance power supply and demand, and reduce the reliance on conventional energy sources. The research also explores strategies for energy storage control, ensuring that storage systems are efficiently charged and discharged based on grid requirements and renewable energy availability, thereby supporting the long-term sustainability and resilience of microgrid systems.

1. Components of the studied microgrid

The power system shown in Fig. 1 consists of two primary components: the AC and the DC sides, which are interconnected using Voltage Source Converters (VSCs) to enable efficient power flow between them. Each side supports different energy sources and storage technologies, intending to balance generation, storage, and consumption to ensure grid stability and optimize energy usage.

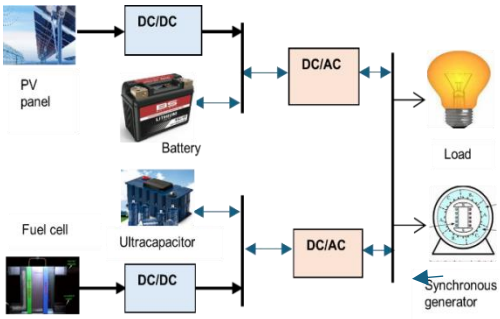

Fig. 1. Microgrid diagram [8]

1.1. DC Side

1.1.1. Photovoltaic generator (PV)

The DC side is equipped with a photovoltaic (PV) array that converts solar energy into direct current (DC) electricity. The output of the PV system varies with sunlight availability, making it a renewable and intermittent source of power. The modeling of a solar PV module follows the same methodology as that used for a solar cell [8, 30]. The simplified principle of a solar panel is illustrated in Fig. 2.

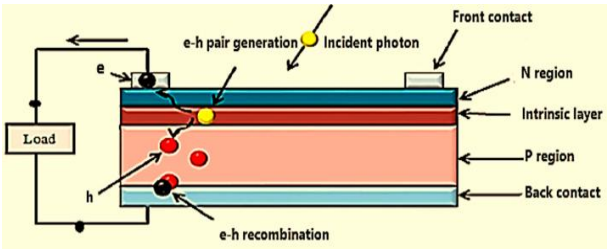

Fig. 2. Photovoltaic solar cell [1]

The MPPT (Maximum Power Point Tracking) controller is used to optimize the power generation from the PV array, ensuring that it operates at its peak efficiency.

In this research the Incremental Conductance (IC) MPPT method is used, it's an advanced algorithm used to accurately track the Maximum Power Point (MPP) of photovoltaic (PV) systems by analyzing the slope of the power-voltage (P-V) curve.

1.1.2. Fuel cell system

A fuel cell system represented in Fig. 3 generates DC power, typically from hydrogen or other fuels. It acts as a reliable and steady power source, complementing the intermittent nature of solar power. The fuel cell can also act as a backup source when the solar output is low or during cloudy conditions [22].

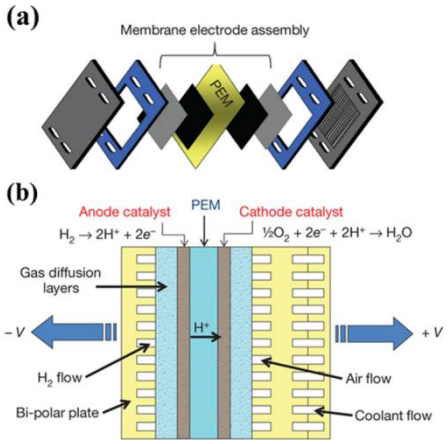

Fig. 3. Fuel cell system components [10]

1.1.3. Energy storage system

Ultracapacitors provide high power density and rapid charge/discharge cycles, which are suitable for addressing short-term power fluctuations and enhancing transient stability. Fig. 4 presents the different components of an ultracapacitor.

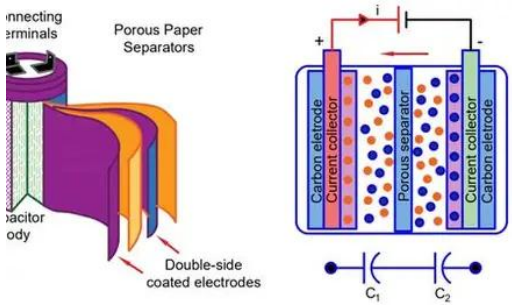

Fig. 4. Construction of the ultracapacitors [32]

Batteries (such as lithium-ion) are used for longer-term energy storage. They store excess energy generated during high production periods (e.g., during the day for PV) and discharge it when demand exceeds supply or when renewable energy production is low.

1.1.4. Voltage source converter (VSC)

The VSCs are critical components for coupling the DC side with the AC side. They enable bidirectional power flow, allowing energy to be supplied from DC sources (such as the PV array, fuel cell, or storage systems) to the AC side and vice versa.

The VSCs also regulate voltage and ensure smooth power conversion, which is crucial for maintaining system stability and ensuring that power quality is maintained. The simplified electrical circuit of the VSC is given in Fig. 5.

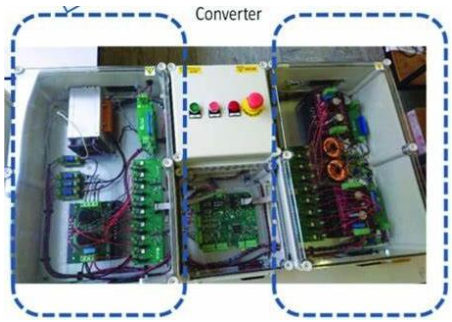

Fig. 5. Voltage source converter hardware [5]

1.2. AC side

1.2.1. Variable AC load

The AC load represents the electricity consumption of the end users connected to the grid, such as residential or industrial facilities. The load can vary over time depending on demand, creating fluctuations that need to be balanced by the generation and storage systems.

The system should be capable of dynamically responding to these changes in demand, ensuring that there is enough generation and storage available to meet the load at all times.

1.2.2. Synchronous generator

The synchronous generator provides additional power generation on the AC side. It could be a traditional generator or a renewable-based system such as a wind turbine. The generator is connected to the grid and serves to stabilize the AC side by providing or absorbing power as needed.

It may operate in grid-connected mode when the microgrid is synchronized with the main grid or in island mode when it operates independently.

1.3. Bidirectional power flow control

The principle of bidirectional power flow control in AC/DC microgrids revolves around enabling seamless energy exchange between the AC and DC subsystems to optimize energy utilization and maintain system stability. This is achieved using Voltage Source Converters (VSCs), which act as the interface between the two systems. The VSCs regulate the direction and magnitude of power flow based on real-time demand and supply conditions. When excess renewable energy is generated on the DC side (e.g., from solar PV or fuel cells), the VSC channels power to the AC side to meet loads or export to the grid. Conversely, during high AC demand or insufficient DC generation, the VSC allows power from the AC grid or synchronous generator to flow into the DC subsystem to support loads or charge storage devices. Advanced control algorithms, including proportional-integral controllers and predictive methods, ensure precise voltage, current, and frequency regulation, enabling efficient, reliable, and bidirectional energy transfer across the microgrid.

2. Equivalent electrical circuits and simulation parameters

The Table 1 given below shows different equivalent circuits used in the modeling of the different components of the microgrid.

Table 1 (part 1). Equivalent circuit of microgrid components

Component	Equivalent circuit	Ref.
PV generator	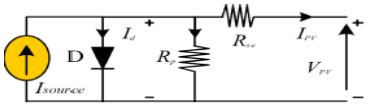	[8]
Fuel cell system	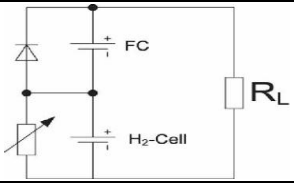	[17]
Batteries	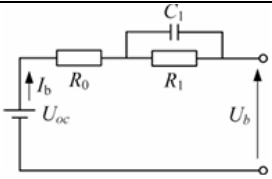	[6]

Table 1 (part 2). Equivalent circuit of microgrid components

Component	Equivalent circuit	Ref.
Ultracapacitor	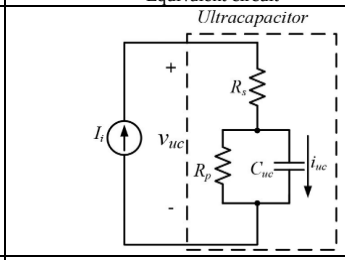	[33]
VSC	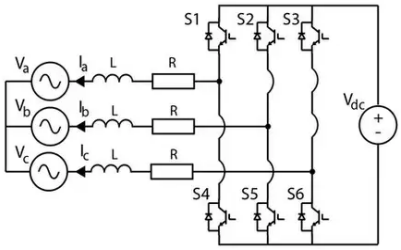	[5]
Synchronous generator	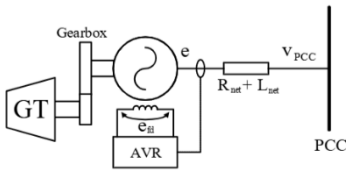	[19]

This Table 2 encapsulates the key simulation parameters for various components, including the voltage source converters (VSC1, VSC2), generator model, ultracapacitor system, photovoltaic system, fuel cell, and battery model.

Table 2. Simulation parameters

Component	Parameter	Value	Unit
VSC1 (Voltage Source Converter 1)	Resistance (R1)	0.02	Ohm
	Inductance (L1)	0.04	H
	Reactance (Xl1)	0.01508	Ohm
	Proportional constant (kp_PQ2)	0.01	-
	Integral constant (ki_PQ1)	0.5	-
VSC2 (Voltage Source Converter 2)	Resistance (R2)	0.02	Ohm
	Inductance (L2)	0.04	H
	Reactance (Xl2)	0.01508	Ohm
	Current integral contant (ki2)	50	-
	Current proportional constant (kp2)	100	-
	Proportional constant (kp_PQ2)	0.01	-
	Integral constant (ki_PQ2)	0.5	-
Generator Model (SM)	Stator parallel resistance (Rl)	1e6	Ohm
	Frequency (f)	60	Hz
	Stator resistance (Rs)	1.0e-3	Ohm
	Stator inductance (Ls)	150e-6	H
Ultracapacitor (UC) System	Resistance (r1)	0.272	Ohm
	Capacitance (c)	7.8e-3	F
	Resistance (r2)	13.53	Ohm
	Voltage (v0)	250	V
	Nominal voltage (vnom)	270	V
Photovoltaic (PV) System	Standard conditions (Gn)	1000	W/m²
	Cell temperature (T)	298.15	°C
	Short-circuit current (Ipvn)	3.45	A
	Open-circuit voltage (Vocn)	21.7	V
	Series resistance (Rs)	0.5	Ohm
	Temperature coefficient (Ki)	0.0014	A/°C
	Temperature coefficient (Kv)	-0.076	V/°C
Fuel Cell (FC)	Internal resistance (Rfc)	20e-3	Ohm
	Internal inductance (Lfc)	1e-2	H
	Proportional gain (kp)	5	-
	Integral gain (ki)	1	-
Battery Model	Internal voltage (kEm)	0.3897	V
	Initial voltage (Em0)	2.2872	V
	Nominal discharge time (T1)	2000	seconds
	Number of cells (ncell)	166	-
	Series resistance (r0)	2.3e-3	Ohm
	Parallel resistance (r1)	1.97e-3	Ohm
	Initial state of charge (SOC0)	0.9	-
	Nominal charge (Qnom)	45	Ah

3. Results and discussion

In this section, we will present the active and reactive powers of the PV system, VSC, load, and synchronous generator (SG), along with the state of charge and voltage of the batteries and ultracapacitors over time.

Fig. 6a illustrates the active power output P (in kilowatts) of a PV system as a function of time (in seconds). Initially, the power output is close to 0 kW, gradually increasing to approximately 1 kW by 50 seconds. The power continues to rise steeply, reaching a peak of around 7 kW at 100 seconds. After this point, the power decreases symmetrically, returning to near 0 kW at around 200 seconds. This indicates a triangular power profile over time.

Fig. 6b illustrates the active power output of the synchronous generator over time. Initially, the generator maintains a steady power output of approximately 5 kW. Around 50 seconds, the power output starts to decline sharply, reaching 0 kW at about 100 seconds. Following this, the generator reverses its role, briefly entering a negative power range, indicating possible power absorption or motoring behavior. After 100 seconds, the power output recovers sharply, peaking at approximately 6.5 kW by 200 seconds, before slightly decreasing. This pattern reflects the generator's dynamic response to load variations or grid conditions, adjusting its operation to ensure system stability and meet energy demands effectively.

Fig. 6c illustrates the active power consumption of the load over time. Initially, the load consumes approximately Initially, the load consumes approximately 5.5 kW. The power consumption increases steadily, reaching around 7 kW at 100 seconds. Beyond this point, the load continues to rise, peaking at approximately 9.5 kW at 180 seconds. After reaching its maximum, the power consumption decreases sharply, dropping back to 5.5 kW by 200 seconds. This trend indicates that the load's power demand fluctuates significantly over time, likely due to operational changes or varying energy requirements of connected devices.

The graph in Fig. 6d illustrates the active power output of the fuel cell over time. At the initial instant (0 s), the fuel cell power is approximately 0 kW. From 0 to 100 seconds, the power output gradually increases, reaching nearly 1.3 kW. Between 100 and 170 seconds, the output continues to rise, peaking at about 2 kW. After 170 seconds, the power decreases sharply, dropping to around 0.3 kW by 230 seconds. This behavior reflects the dynamic response of the fuel cell: a progressive ramp-up during the start-up phase, followed by a peak operating point, and then a decline that may correspond to load reduction, fuel supply variation, or control system regulation to stabilize operation.

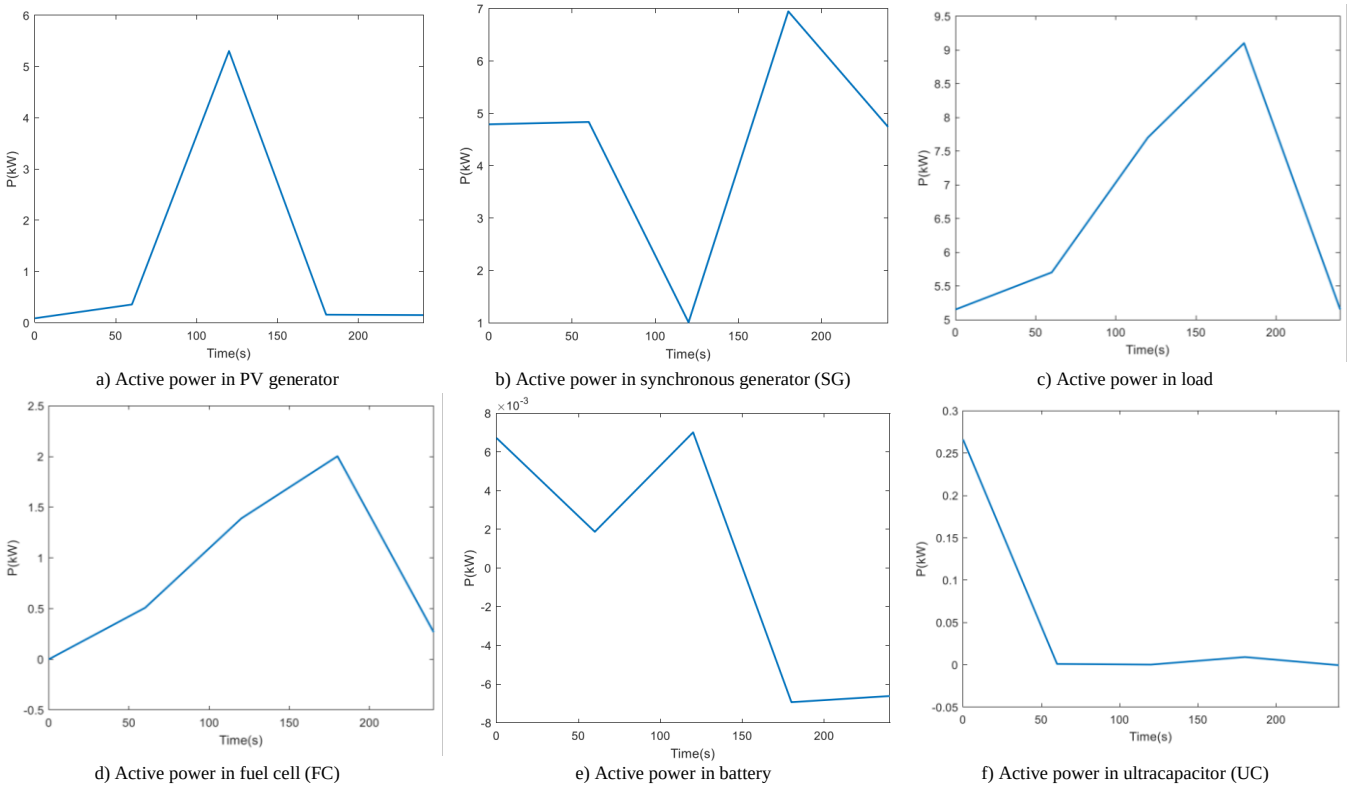

a) Active power in PV generator
b) Active power in synchronous generator (SG)
c) Active power in load
d) Active power in fuel cell (FC)
e) Active power in battery
f) Active power in ultracapacitor (UC)

Fig. 6. Active power in different components of the microgrid

In Fig. 6e, the graph depicts the active power behavior of the battery over time. Initially, the battery discharges with a power output of approximately 6.5×10^{-3} kW. Within the first 50 seconds, the power output decreases to around 2×10^{-3} kW. Between 50 and 120 seconds, the discharge increases again, reaching nearly 7×10^{-3} kW. Beyond 120 seconds, the battery transitions into a charging state with negative values, dropping steeply to about -7×10^{-3} kW at 180 seconds. Toward the end of the simulation (200–230 s), the charging slightly decreases in magnitude, stabilizing near -6.5×10^{-3} kW.

This pattern highlights the battery's role in dynamically managing energy by alternating between charging and discharging, likely in response to system demands or control strategies. The relatively low values of power indicate that the battery is either being charged or discharged at a low rate, which could be due to several factors: the renewable energy sources (PV) in the hybrid system might be providing sufficient power to meet the demand, leading to minimal use of the battery; alternatively, it could indicate a low-load demand, where the battery is not required to supply much power. A consistent low power value can also point to the battery being used for balancing minor fluctuations in power generation or consumption rather than large-scale energy storage or delivery. In this context, the observed low power values reflect the system's efficiency in balancing energy supply and demand with minimal reliance on battery storage, suggesting optimal operation where renewable energy sources sufficiently meet the load requirements and the battery only assists when necessary.

The graph in Fig. 6f illustrates the active power profile of the ultracapacitor over time. Initially, the ultracapacitor discharges with a power output of approximately 0.25 kW at the start. Within the first 50 seconds, the power decreases

rapidly, approaching 0 kW. After this point, the power output remains nearly zero, with minor fluctuations observed up to 200 seconds. This behavior indicates that the ultracapacitor is primarily utilized for an initial discharge, likely to handle a transient demand or power surge, and subsequently transitions to a low-activity state, maintaining stability within the system.

Fig. 7a depicts the reactive power consumption of the load over time. Initially, the load consumes approximately –0.5 kvar. The reactive power gradually decreases, reaching around –0.65 kvar by 50 seconds. Beyond this point, the consumption continues to drop, hitting its minimum of approximately –0.95 kvar at 120 seconds. Following this, the reactive power increases sharply, returning to approximately –0.55 kvar by 200 seconds. The negative values throughout the graph indicate that the load exhibits an inductive characteristic, typical of equipment such as motors or transformers. The observed fluctuations likely reflect changes in the operating conditions or the number of active devices within the system.

Fig. 7b illustrates the variation of reactive power (Q, in kvar) in a synchronous generator over time (in seconds). The reactive power fluctuates throughout the interval, starting at approximately –0.35 kvar, increasing slightly to about –0.4 kvar around t = 50 seconds, then dropping significantly to nearly –0.65 kvar at t = 150 seconds, before rising again to approximately –0.35 kvar by t = 200 seconds. These dynamics likely represent changes in the generator's load or excitation system, impacting its ability to supply or absorb reactive power to maintain voltage stability in the connected electrical grid. Precise numerical values are crucial for optimizing reactive power compensation strategies and ensuring efficient grid operation.

The graph represents in Fig. 7c show the reactive power (Q in kvar) behavior of a voltage source converter (VSC1) over time. Initially, Q starts at around –0.11 kvar and shows a slight decline to approximately –0.13 kvar at 50 seconds. The reactive power then decreases more sharply, reaching a minimum value of about –0.18 kvar around 150 seconds. Subsequently, Q rises significantly, returning to approximately –0.11 kvar by 200 seconds. This trend may reflect the VSC's dynamic response to changing grid demands, such as varying load conditions or voltage control efforts, showcasing its role in managing reactive power for grid stability.

The reactive power (Q in kvar) profile is presented in Fig. 7d of a voltage source converter (VSC2) over time. Initially, Q is approximately –0.05 kvar and declines slightly to around –0.06 kvar at 50 seconds. Following this, the reactive power drops sharply, reaching a minimum of about –0.09 kvar at around 150 seconds. Afterward, Q increases steeply, returning to nearly –0.05 kvar by 200 seconds. This behavior indicates the VSC's role in dynamically compensating for reactive power changes in the system, ensuring grid voltage stability and managing power flow efficiently under varying conditions.

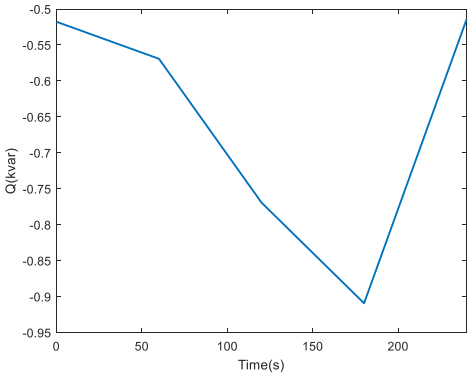

a) Reactive power in load

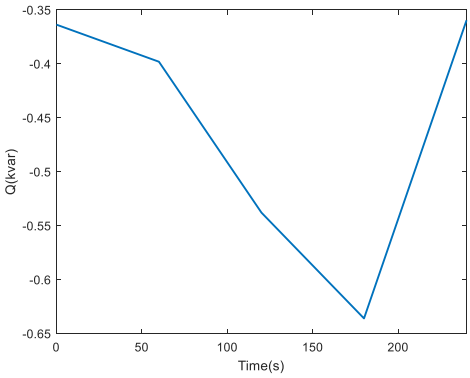

b) Reactive power in SG

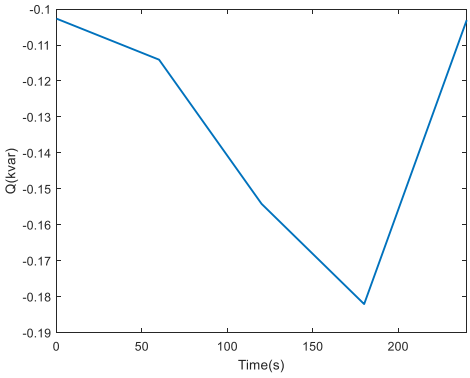

c) Reactive power in VSC1

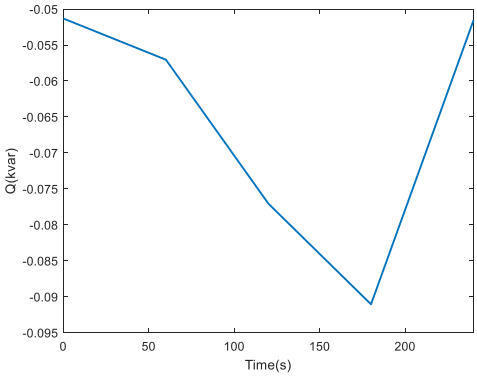

d) Reactive power in VSC2

Fig. 7. Reactive power in different components of the microgrid

Fig. 8a illustrates the state of charge (SOC) of a battery as a percentage over time (in seconds). Initially, the SOC remains constant at 90% for the first 50 seconds, indicating no discharge. After this period, the SOC starts to decrease steadily, reaching approximately 89.9992% by 250 seconds. This trend suggests a controlled and slow discharge process over time, possibly due to a low power load.

Fig. 8b shows the state of charge (SOC) of a battery as a percentage over time (in seconds). The SOC starts at approximately 85.43% and gradually decreases over the observation period, reaching about 85.33% by 250 seconds. This indicates a steady discharge of the battery, with a small, consistent drop in SOC over time, suggesting either a low discharge rate or minimal power draw during this period.

In Fig. 9a, the battery voltage remains nearly constant throughout the simulation, reflecting stable operating conditions. At the initial instant (t = 0 s), the voltage is about 431.653 V. By 60 seconds, it increases slightly to 431.658 V, then shows a minor dip to 431.657 V around 120 seconds. From 120 to 170 seconds, the voltage rises gradually to a peak of 431.667 V, before settling slightly lower at 431.666 V toward 230 seconds. The extremely narrow variation range of roughly 0.015 V confirms that the battery operates under well-regulated conditions, with minimal voltage fluctuations during charging and discharging cycles.

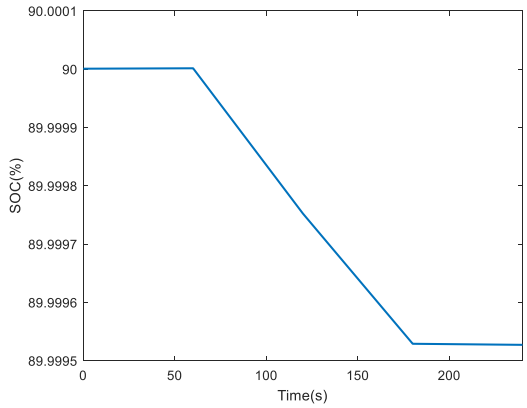

a) State of charge (SOC) in battery

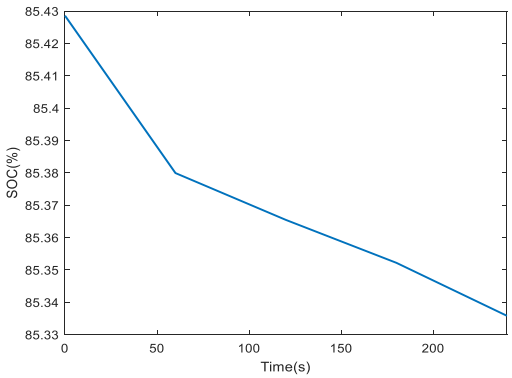

b) State of charge (SOC) in ultracapacitor

Fig. 8. State of charge in batterie.

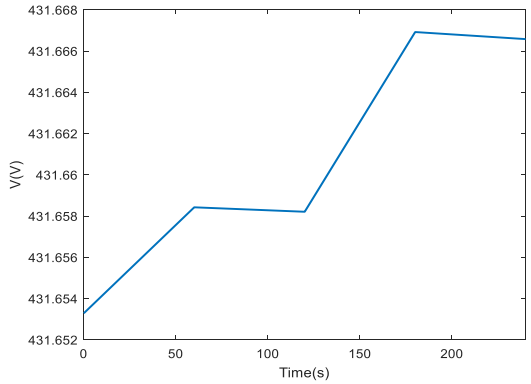

a) Voltage in battery

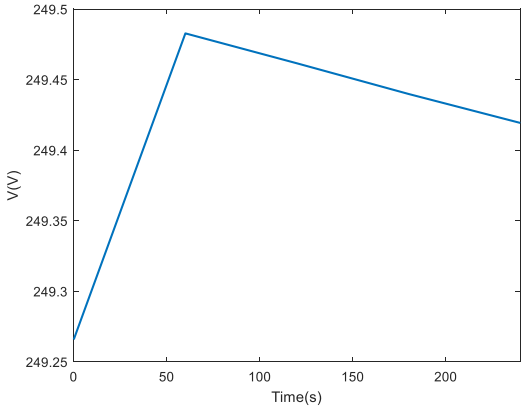

b) Voltage in ultracapacitor

Fig. 9. Voltage in battery and ultracapacitor

The voltage profile of the ultracapacitor (Fig. 9b) shows a rapid initial increase from about 249.27 V at the start to a peak of roughly 249.48 V within the first 60 s, indicating the fast charging response typical of ultracapacitors due to their high power density. After reaching the peak, the voltage gradually decreases over time, settling near 249.42 V at around 230 s, which suggests a slight self-discharge or redistribution of charge within the device. Overall, the curve highlights the ultracapacitor's quick voltage response during charging and its relatively stable but slightly decaying voltage behavior during the following period.
The stable voltage profiles of both the battery and the ultracapacitor highlight the robustness of the system, ensuring reliable operation under varying conditions and confirming its capability to support dynamic energy demands.

4. Conclusion

The analysis of active power dynamics in the microgrid reveals the complementary roles of its components in ensuring system stability and reliability. The photovoltaic (PV) system follows a triangular power profile, with output starting at zero, peaking at 7 kW at the midpoint, and returning to zero within a 200-second interval, reflecting its reliance on external factors like sunlight. The synchronous generator's power output fluctuates between –1 kW and 7 kW, responding to load demand variations, transient events, and stability challenges. The load's active power consumption ranges from 5.5 kW to 9.5 kW, indicating dynamic operational changes driven by connected equipment.

The fuel cell generates power between 0 kW and 2 kW, with negative values during startup or shutdown processes, illustrating its ability to adapt to varying operating conditions. The battery alternates between charging (negative power) and discharging (positive power), effectively managing energy demand and contributing to system control. Similarly, the ultracapacitor's rapid charge and discharge cycles, ranging from –0.05 kW to 0.3 kW, play a crucial role in stabilizing the system during power spikes or drops. Together, these components form a coordinated system where energy generation, storage, and load balancing work in unison to ensure stability and reliability under changing conditions.

Reactive power management is also vital for maintaining voltage regulation and system stability within the microgrid. The load exhibits inductive characteristics, consuming reactive power from –0.95 kvar to –0.5 kvar, which fluctuates with operational changes like varying device states or connected equipment. The synchronous generator contributes reactive power, with output levels between –0.65 kvar and –0.35 kvar, helping stabilize the grid through excitation control. Voltage source converters (VSC1 and VSC2) also supply reactive power, with VSC1 providing –0.19 kvar to –0.1 kvar, and VSC2 supplying –0.095 kvar to –0.05 kvar, demonstrating their dynamic reactive power support in response to grid conditions and load demands.

The voltage profiles of the battery and ultracapacitor confirm the system's effective energy management. The battery voltage remains stable, fluctuating narrowly between 431.653 V and 431.667 V over 230 seconds, while the ultracapacitor's voltage shows slight variations between 249.27 V and 249.48 V. These stable voltage levels underscore the system's ability to balance charging and discharging efficiently, ensuring optimal performance and long-term reliability.

Compared with existing approaches, the proposed microgrid strategy provides notable improvements. The coordinated action of PV, fuel cell, battery, ultracapacitor, and synchronous generator reduces active power fluctuations and ensures reliable load following. At the same time, effective reactive power management from the generator and VSC units maintains voltage regulation. The stability of battery and ultracapacitor voltages confirms efficient charge–discharge coordination, enhancing long-term reliability. Overall, the results highlight that our integrated control method achieves superior stability, adaptability, and efficiency compared to conventional methods.

In conclusion, the microgrid's active and reactive power dynamics are governed by the seamless integration of its components. Renewable energy generation from the PV system and fuel cell is complemented by energy storage and rapid response capabilities of the battery and ultracapacitor.

The synchronous generator maintains a stable power supply, while coordinated control strategies manage the variable load demands. This interplay ensures adaptability to changing conditions, maintaining efficiency, stability, and voltage regulation through effective reactive power management.

References

[1] Al-Ezzi A. S., Ansari M. N. M.: Photovoltaic Solar Cells: A Review. Applied Systems Innovation 5(4), 2022, 67 [https://doi.org/10.3390/asi5040067].
[2] Al-Ismail F. S.: DC Microgrid Planning, Operation, and Control: A Comprehensive Review. IEEE Access 9, 2021, 36154–36172 [https://doi.org/10.1109/ACCESS.2021.3062840].
[3] Alam M. S. et al.: Renewable Energy Integration with DC Microgrids: Challenges and Opportunities. Electric Power Systems Research 234, 2024, 110548 [https://doi.org/10.1016/j.epsr.2024.110548].
[4] Atawi I. E. et al.: Recent Advances in Hybrid Energy Storage System Integrated Renewable Power Generation: Configuration, Control, Applications, and Future Directions. Batteries 9(1), 2023, 29 [https://doi.org/10.3390/batteries9010029].
[5] Baker N. et al.: Development and Wave Tank Demonstration of a Fully Controlled Permanent Magnet Drive for a Heaving Wave Energy Converter. Energies 15(13), 2022, 4811 [https://doi.org/10.3390/en15134811].
[6] Bašić M. et al.: Dynamic Equivalent Circuit Models of Lead-Acid Batteries: A Performance Comparison. IFAC-PapersOnLine 55(4), 2022, 189–194 [https://doi.org/10.1016/j.ifacol.2022.06.031].
[7] Bharti K. P. et al.: Designing a Bidirectional Power Flow Control Mechanism for Integrated EVs in PV-Based Grid Systems Supporting Onboard AC Charging. Sustainability 16(20), 2024, 8791 [https://doi.org/10.3390/su16208791].
[8] Boumous Z., Boumous S.: Novel Intelligent Control of Photovoltaic System Using ANFIS Gravitational Search for MPPT Controller. Przegląd Elektrotechniczny 100(7), 2024, 108–112.
[9] Cagnano A., De Tuglie E., Mancarella P.: Microgrids: Overview and Guidelines for Practical Implementations and Operation. Applied Energy 258, 2020, 114039 [https://doi.org/10.1016/j.apenergy.2019.114039].
[10] Cao F. et al.: Advances in Low Pt Loading Membrane Electrode Assembly for Proton Exchange Membrane Fuel Cells. Molecules 28(2), 2023, 773 [https://doi.org/10.3390/molecules28020773].
[11] Choudhury S.: Review of Energy Storage System Technologies Integration to Microgrid: Types, Control Strategies, Issues, and Future Prospects. Journal of Energy Storage 48, 2022, 103966 [https://doi.org/10.1016/j.est.2022.103966].
[12] Di Piazza M. C.: Energy Management Systems for Optimal Operation of Electrical Micro/Nanogrids. Energies 14, 2021, 8469 [https://doi.org/10.3390/en14248469].
[13] Faazila Fathima S., Premalatha L.: Protection Strategies for AC and DC Microgrid – A Review of Protection Methods Adopted in Recent Decade. IETE Journal of Research 69(9), 2021, 6573–6589 [https://doi.org/10.1080/03772063.2021.1990140].
[14] Fu Q. et al.: Dynamic Analysis of Energy Storage Integrated Systems Considering Bidirectional Power Flow and Different Control Loops of Energy Storages. Journal of Energy Storage 86, 2024, 111171 [https://doi.org/10.1016/j.est.2024.111171].
[15] Gao T., Lu W.: Machine Learning Toward Advanced Energy Storage Devices and Systems. iScience 24(1), 2021, 101936 [https://doi.org/10.1016/j.isci.2020.101936].
[16] Gundogdu B., Gladwin D. T.: Bi-Directional Power Control of Grid-Tied Battery Energy Storage System Operating in Frequency Regulation. International Electrical Engineering Congress (iEECON), IEEE, 2018, 1–4 [https://doi.org/10.1109/IEECON.2018.8712259].
[17] Hahn R. et al.: Optimization of Efficiency and Energy Density of Passive Micro Fuel Cells and Galvanic Hydrogen Generators. Design, Test, Integration & Packaging of MEMS/MOEMS (DTIP), 2008, 34–41 [https://doi.org/10.1109/DTIP.2008.4752947].
[18] Hannan M. A. et al.: Power Electronics Contribution to Renewable Energy Conversion Addressing Emission Reduction: Applications, Issues, and Recommendations. Applied Energy 251, 2019, 113404 [https://doi.org/10.1016/j.apenergy.2019.113404].
[19] Kalitjuka T.: Control of Voltage Source Converters for Power System Applications. Master's thesis. Norwegian University of Science and Technology 2011.
[20] Malekjamshidi Z. et al.: Bidirectional Power Flow Control with Stability Analysis of the Matrix Converter for Microgrid Applications. International Journal of Electrical Power & Energy Systems 110, 2019, 725–736 [https://doi.org/10.1016/j.ijepes.2019.03.053].
[21] Nair U. R., Costa-Castelló R.: A Model Predictive Control-Based Energy Management Scheme for Hybrid Storage System in Islanded Microgrids. IEEE Access 8, 2020, 97809–97822 [https://doi.org/10.1109/ACCESS.2020.2996434].
[22] Plait A., Saenger P., Bouquain D.: Fuel Cell System Modeling Dedicated to Performance Estimation in the Automotive Context. Energies 17(15), 2024, 3850 [https://doi.org/10.3390/en17153850].
[23] Qoria T. et al.: Current Limiting Algorithms and Transient Stability Analysis of Grid-Forming VSCs. Electric Power Systems Research 189, 2020, 106726 [https://doi.org/10.1016/j.epsr.2020.106726].
[24] Radhika R., Thampatty K. C. S.: Impacts of Renewable Energy Integration on Power System Stability. Technology & Engineering Management Conference – Asia Pacific (TEMSCON-ASPAC), IEEE, 2023, 1–6 [https://doi.org/10.1109/TEMSCON-ASPAC59527.2023.10531586].
[25] Ramos G. A., Costa-Castelló R.: Energy Management Strategies for Hybrid Energy Storage Systems Based on Filter Control: Analysis and Comparison. Electronics 11(10), 2022, 1631 [https://doi.org/10.3390/electronics11101631].
[26] Ren Z., Du C.: A Review of Machine Learning State-of-Charge and State-of-Health Estimation Algorithms for Lithium-Ion Batteries. Energy Reports 9, 2023, 2993–3021 [https://doi.org/10.1016/j.egyr.2023.01.108].
[27] Sarwar S. et al.: Enhanced Energy Balancing and Optimal Load Curtailment Strategy for DC Microgrid Integration in Hybrid AC/DC Distribution Networks. IET Smart Grid 7(4), 2024, 400–411 [https://doi.org/10.1049/stg2.12164].
[28] Sreenu C. et al.: Pairing Voltage-Source Converters with PI Tuning Controller Based on PSO for Grid-Connected Wind-Solar Cogen. Franklin Open 8, 2024, 100138 [https://doi.org/10.1016/j.fraope.2024.100138].
[29] Stoffel P. et al.: Evaluation of Advanced Control Strategies for Building Energy Systems. Energy and Buildings 280, 2023, 112709 [https://doi.org/10.1016/j.enbuild.2022.112709].
[30] Szpulak P. et al.: Investment Profitability Analysis of an On-Grid Photovoltaic System. Informatyka, Automatyka, Pomiary w Gospodarce i Ochronie Środowiska 7(2), 2017, 36–39 [https://doi.org/10.5604/01.3001.0010.4835].
[31] Tang C., Zhao J.: Distributed Economic Pinning Control Based on Deep Reinforcement Learning for Isolated Microgrids. Electric Power Systems Research 241, 2025, 111377 [https://doi.org/10.1016/j.epsr.2024.111377].
[32] Teasdale A. et al.: A Study on an Energy-Regenerative Braking Model Using Supercapacitors and DC Motors. World Electric Vehicle Journal 15(7), 2024, 326 [https://doi.org/10.3390/wevj15070326].
[33] Tseng K.-C., Chang Y.-C., Cheng C.-A.: Implementation and Analysis of Ultracapacitor Charger in Hybrid Energy-Storage System for Electric-Vehicle Applications. IET Power Electronics 13, 2020, 1–9 [https://doi.org/10.1049/iet-pel.2019.1469].

D.Sc. Zouhir Boumous
e-mail: zohir.boumous@univ-soukahras.dz

Zouhir Boumous is an electrical engineering graduate of the University of Annaba, magister of the University of Annaba, Doctor of Science of the University of Setif, member of the Laboratory of electrical engineering, electronic and renewable energy at the University of Souk Ahras, president of the research project on tolerant control of electrical systems hosted at the University of Souk Ahras, he is the thesis director of several doctorate subjects in fault detection in electrical machines.
His areas of research are: smart grid, tolerant control, machine faults, power electronics.

https://orcid.org/0000-0003-4972-1805

D.Sc. Samira Boumous
e-mail: samira.boumous@univ-soukahras.dz

Samira Boumous is an electrical engineer from the University of Annaba, a magister from the University of Jijel, a Doctor of Science from the University of Setif, a member of the Laboratory of electrical engineering, electronic and renewable energy at the University of Souk Ahras, president of a research project on photovoltaic systems hosted by the University of Souk Ahras, and thesis director of several doctoral dissertations on optimizing and improving power quality in microgrids.
Her research focuses on power quality, smart grids and power electronics.

https://orcid.org/0000-0003-2213-6542

D.Sc. Tawfik Thelaidjia
email: t.thelaidjia@univ-soukahras.dz

Tawfik Thelaidjia received magister degrees from Tebessa University, in 2013. He received a doctorate in sciences degree in electrical engineering from the University of Guelma on 2017. He received the university habilitation degree in electrical engineering from the University of Tebessa on 2021. His research activities include the control, the monitoring and the diagnosis of industrial applications using intelligent algorithms.

https://orcid.org/0000-0003-4222-323X